

DESIGN, SIMULATION AND EXPERIMENTAL ANALYSIS OF WIDEBAND CIRCULARLY POLARIZED CAPACITIVE FED MICROSTRIP ANTENNA

S. Murugan^{1, *} and V. Rajamani²

¹ECE Department K.L.N.College of Engineering, Pottapalayam, Sivagangai District, Tamilnadu 630611, India

²Indra Ganesan College of Engineering, Tiruchirappalli, Tamilnadu 620012, India

Abstract—Wideband Circularly polarized antenna receive much attention in the wireless communication applications such as Global positioning system (GPS) and Personal communication system (PCS). In this paper, a microstrip square patch, truncated in opposite corners, suspended above the ground plane is proposed. The geometry incorporates the capacitive feed strip which is fed by a coaxial probe. The proposed structure is designed, simulated and fabricated to cover the entire frequency of GPS, i.e., L_1 (1.575 GHz), L_2 (1.227 GHz), and L_5 (1.176 GHz), covering from (1.15 GHz–1.6 GHz). The parameters such as return loss, VSWR, impedance, radiation efficiency axial ratio and radiation pattern are used for analyzing the performance of the antenna. Both simulated and experimental results are presented and they exhibit broadband characteristics, covering the desired frequency bands.

1. INTRODUCTION

Microstrip antennas (MSA) in their basic structure radiate linearly polarized waves. The circular polarization (CP) is obtained by modifying the basic geometry of MSA/feed. Microstrip antennas are resonant type, possessing numerous advantages such as light weight, low cost, easy fabrication, moderate gain, but they are inheritance of Bandwidth (BW). The applications of wireless communication such as GPS, mobile phones, satellite communication require more BW (at least 10%) due to integration of various services in single

Received 26 March 2012, Accepted 12 June 2012, Scheduled 16 June 2012

* Corresponding author: Sathiyamoorthy Murugan (murugans1976@gmail.com).

receiver. Circularly Polarized (CP) planar antennas have received much attention for GPS applications. The main advantage of CP is that regardless of receiver orientation, it will receive a component of signal.

Generally, thicker substrates with low dielectric constant give broad bandwidth for MSA [1]. Bandwidth describes the range of frequencies over which certain antenna parameters such as VSWR and radiation pattern are within the specified range. The bandwidth of MSA shall also be enhanced by adding the impedance matching networks, stubs by compensating the reactance part of the input impedance of MSA. But the disadvantage is that adding extra component to the circuit increases the complexity of the structure and also, occupying more space. Alternatively, suspended MSA configuration with capacitive feeding was found in the literature [2–4] to improve the bandwidth of MSA. It was demonstrated [2] that the suspended configuration with capacitive feeding increases the BW up to 50% at centre frequency of 5.9 GHz whereas a conventional MSA exhibits only 1–5% BW. The rectangular patch is used as radiating element in [2, 4]. A triangular shape radiating patch with capacitive feed was discussed in [3]. Irrespective of the shape of the patch, this technique increases the BW of MSA. The increase in operating frequency increases the percentage of fractional BW and vice-versa, e.g.) for 2 GHz operating frequency, the fractional bandwidth obtained was 42% and for 10 GHz, the BW was 58.2% in [2].

The axial ratio is the ratio of orthogonal components of an E -field. A circularly polarized field is made up of two orthogonal E -field components of equal amplitude (and 90 degrees out of phase). Because the components are equal magnitude, the axial ratio is 1 (or 0 dB). The axial ratio for an ellipse is larger than 1 (> 0 dB). The axial ratio for pure linear polarization is infinite, because the orthogonal component of the field is zero. Axial ratios are often quoted for antennas in which the desired polarization is circular. The ideal value of the axial ratio for circularly polarized fields is 0 dB. The design and study of truncated corner wideband circularly polarized antenna was discussed in [5]. The study concludes that the AR BW increases with increase in substrate thickness and also, use of L-probe/U-slot feeding increase the AR BW more than 10%. An axial ratio BW of 14% was reported for the substrate thickness of $0.2\lambda_0$ [5]. A coplanar capacitive fed fractal microstrip antenna was presented to produce wide band circularly polarized beam, an axial ratio BW of 7% was reported in [6]. The same author attempted in [7] to reduce the overall height of a capacitive coupled low profile suspended microstrip antenna, keeping the BW requirement about 30%. Also, it is demonstrated

that the gain and radiation pattern of the proposed antenna remain nearly unchanged. A single feed circularly polarised fractal microstrip antenna with fractal slot was presented in [8]. Recently, a truncated square patch suspended over the ground plane with capacitive feed for obtaining circular polarization and wideband to cover the entire frequency of GPS (1.15–1.6 GHz) was discussed in [9]. The simulation results showed better axial ratio BW of 16% and impedance BW of 32% in [9]. The axial ratio BW is substantially more than earlier reported results in [5, 6]. Particularly, for GPS applications, few papers were found in literature [10–16].

In this paper, a wide band circularly polarized truncated square microstrip antenna with capacitive feeding is designed, simulated and fabricated. The paper is organized as follows: Section 2 covers the design methodology, Section 3 presents the simulation studies, Section 4 presents experimental results and Section 5 concludes the paper.

2. DESIGN METHODOLOGY

The top view and side view of the proposed truncated square patch antenna geometry is shown in Fig. 1.

It is basically a suspended coplanar capacitive fed microstrip antenna. The microstrip antenna is generally fed by coaxial probe, microstrip line feeding, aperture coupling method and electromagnetic

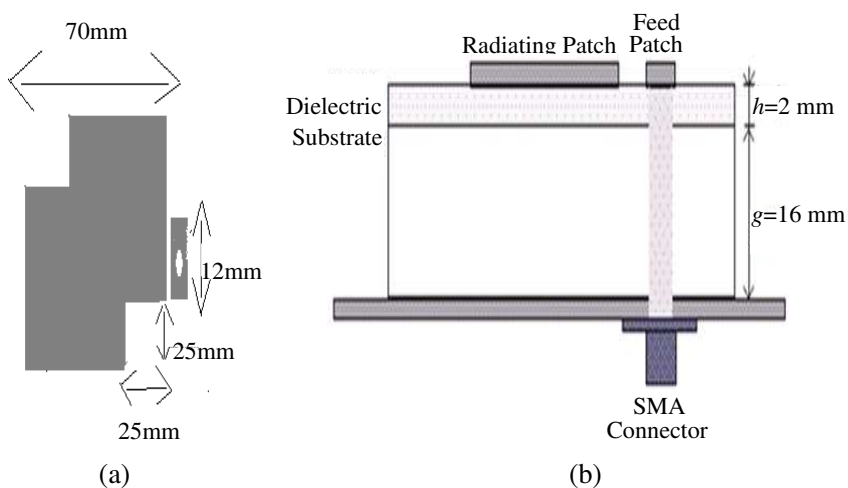


Figure 1. (a) Top view (b) cross sectional view of the square patch antenna with capacitive probe feed.

coupling. In capacitive feeding method, a small feed patch is placed very close to the actual radiating patch. The antenna is excited by connecting a coaxial probe to the feed strip by a long pin SMA connector. The feed strip electromagnetically couples the energy to the radiating patch element. This method is advantageous because (i) it compensates the reactance produced by the inductance of the long probe and better impedance matching at desired frequencies (ii) both radiating patch and the feed strip can be etched on the same dielectric substrate. The substrate and ground plane are separated by an air gap with height (g). The key design parameters of the above antenna include air gap (g), separation between radiator strip and feed strip (d), and length (t) and width (s) of feed strip. FR4 substrate with dielectric constant 4.4 and thickness 2 mm is used for antenna fabrication. Though it is a lossy substrate, the antenna parameters are optimized at design frequency. Also, FR4 is cheaper and easily available than other substrates.

The antenna was designed to operate with a center frequency of 1.375 GHz. The radiator patch dimensions can be calculated from standard design expressions found in [17, 18] after making necessary corrections for the suspended ($g + h$) dielectric. All parameters are optimized using commercially available electromagnetic software.

$$W = 1/2f_r \sqrt{g\mu_0\varepsilon_0}[\sqrt{2/\varepsilon_r + 1}] \quad (1)$$

$$\varepsilon_{reff} = (\varepsilon_r + 1)/2 + (\varepsilon_r - 1)/2[1 + 12h/W]^{-1/2} \quad (2)$$

$$\Delta L/h = 0.412(\varepsilon_{reff} + 0.3)(W/h + 0.264)/(\varepsilon_{reff} - 0.258)(W/h + 0.8) \quad (3)$$

$$L_{eff} = 1/2f_r \sqrt{\varepsilon_{reff}} \sqrt{\mu_0\varepsilon_0} \quad (4)$$

$$L = L_{eff} - 2\Delta L \quad (5)$$

The equivalent dielectric constant for the above air-dielectric geometry antenna is calculated by using the principle of capacitance between two dielectrics (air-FR4) [17]

$$\varepsilon_{eq} = \varepsilon_r(h + g)/(\varepsilon_r g + h) \quad (6)$$

In all the above Equations (2)–(6), the dimensions are found by replacing ε_r value by ε_{eq} . Use of air-gap enhances the bandwidth without increasing the lateral size and complexity of the antenna too much. It has been shown that impedance bandwidth of an antenna may be maximized by the design expressions [17, 18]

$$g = 0.16\lambda_0 - h\sqrt{\varepsilon_r} \quad (7)$$

where, g = height of air gap,

h = thickness of the substrate,

ε_r = relative permittivity of the dielectric,

$\varepsilon_{re\text{ff}}$ = effective dielectric constant,
 $\Delta L/h$ = Normalized line extension,
 ε_{eq} = equivalent dielectric constant for air-dielectric geometry,
 W = width of the radiating patch,
 L = Length of the radiating patch,
 L_{eff} = Effective length,
 λ_0 = wavelength.

The minimum possible width of the feed strip is 2.4 mm so that a hole can be made to connect the probe pin. The minimum separation between the patch and the feed strip is 0.5 mm. The size of the feed patch ('t' and 's') and the gap between the two patches are varied to adjust the input impedance. The feed patch dimensions are optimized for better performance.

Circular polarization is achieved by truncating a square of size 70 mm in the two opposite square corners. The antenna parameters are optimized by varying the size of truncated square corners and finally, it is seen that a square size of 25 mm is truncated in two opposite corners yields the optimized results at the design frequency (Table 1). Initially, the truncated square is kept as 20 mm and gradually it is increased to 25 mm, 30 mm and simulations were repeated by keeping other parameters constant.

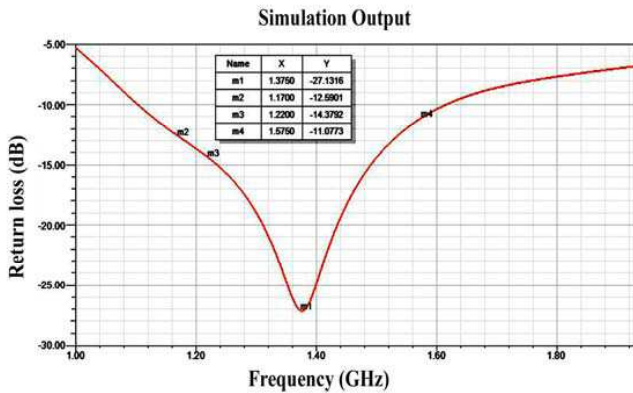
From Table 1, the size of truncated square is chosen as 25 mm. At this value, the axial ratio is reaching minimum value of 0.031 dB. Further, it is inferred from the Table 1, the increase in size of truncated square patch causes (i) Shifts the resonant frequency from lower value to higher value (ii) Decrease in Impedance BW (iii) Decrease in Gain

Table 1. Optimization of truncated square patch size.

Truncated square size	Resonant frequency/ Return loss (dB)	Impedance BW (< -10 dB)	Gain (dB)	Minimum Axial ratio/ Frequency
20 mm	1.26 GHz / -25.7	1.10–1.76 GHz (0.66 GHz)	2.9	4.2 dB /1.395 GHz
25 mm	1.375 GHz / -27	1.15–1.6 GHz (0.45 GHz)	2.1	0.03 dB /1.375 GHz
30 mm	1.43 GHz / -25.4	1.25–1.62 GHz (0.37 GHz)	0.8	3.6 dB /1.30 GHz

Table 2. Final dimensions for the antenna design.

Parameter	Value
Size of original square patch	70 mm
Size of the truncated corner square	25 mm
Length of the feed strip, s	12 mm
Width of the feed strip, t	2.4 mm
Separation of feed strip from patch	0.5 mm
Air gap, g	16.0 mm
Substrate thickness, h	2 mm
Dielectric constant	4.4

**Figure 2.** Return loss Vs frequency.

of radiation pattern in the bore sight axis (iv) Axial ratio value shifts from high resonant frequency to low resonant frequency.

The final dimensions of the proposed antenna are shown in Table 2 above.

3. SIMULATION STUDIES

The simulation results for parameters such as return loss (dB), VSWR radiation pattern, input impedance, axial ratio and radiation efficiency as a function of frequency are presented in Figs. 2–7.

Figure 2 shows the return loss variation with respect to frequency of the antenna. Return loss may be defined as the difference in dB between the power sent towards the antenna-under-test (AUT)

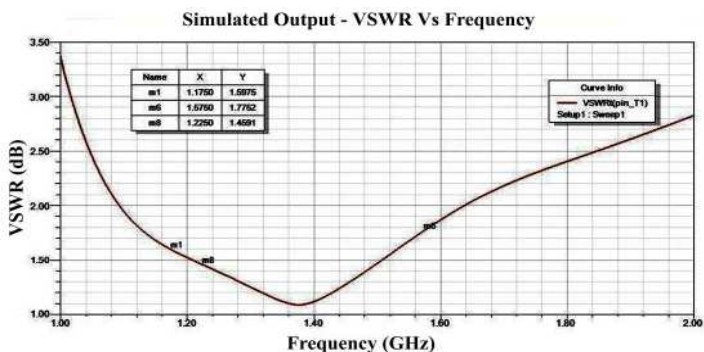


Figure 3. Simulated VSWR Vs frequency.

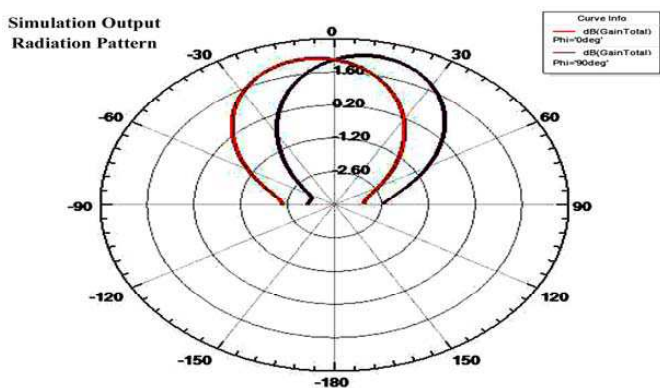


Figure 4. Radiation pattern in the principal planes ($\varphi = 0$ and $\varphi = 90$).

and power reflected [19]. The requirement for reflection coefficient for wireless devices specifies 10 dB return loss BW. The proposed antenna shows wide impedance BW starting from 1.15 to 1.6 GHz. i.e., 0.45 GHz. The percentage BW is 32% at centre frequency 1.375 GHz. This value satisfies our required BW for covering L_1 , L_2 and L_5 frequencies of operation.

Figure 3 shows the simulated VSWR Vs frequency plot. In the desired operating frequencies, the VSWR is less than two. Hence, the impedance matching is good at these frequencies.

Figure 4 shows the radiation pattern of wide band GPS antenna. The radiation pattern show a hemispherical radiation pattern in both the principal planes $\varphi = 0$ and $\varphi = 90$. The Gain value is 2.1 dB in the bore-sight axis of the antenna. The gain variation over the main lobe is around 5 dB.

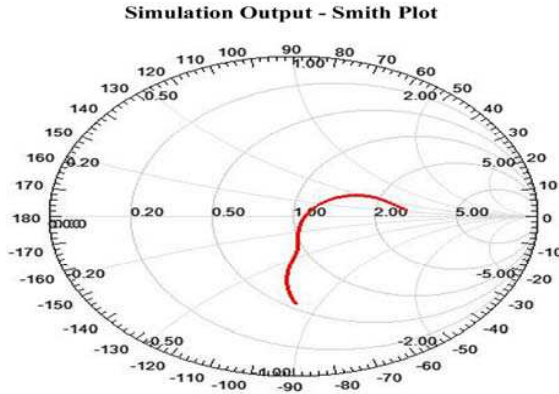


Figure 5. Simulated normalised input impedance Vs frequency.

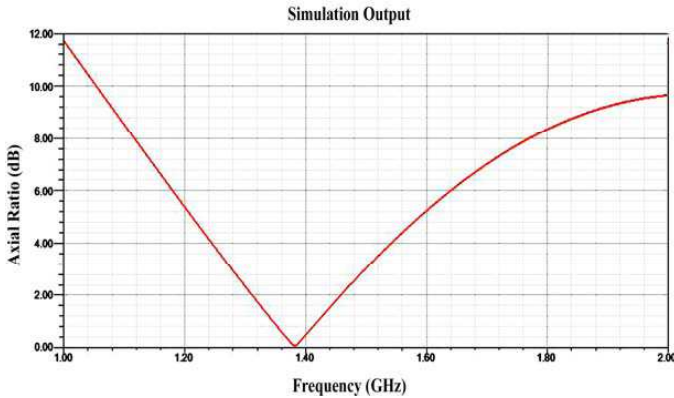


Figure 6. Axial ratio Vs frequency.

Figure 5 shows the input impedance of the designed antenna. The coaxial cable has normally a characteristic impedance of $50\ \Omega$. In the simulation, characteristic impedance of $50\ \Omega$ is taken for impedance matching. At resonance, the input impedance of the antenna should have only real part and negligible imaginary part. The impedance curve is inside the unity circle, crossing the circle at 1.3 GHz. Hence the designed antenna satisfies the impedance matching condition.

Figure 6 shows the axial ratio performance of antenna. A circularly polarized antenna should have an axial ratio of less than 3 dB at the design frequency. In this design, the axial ratio is less than 3 dB between 1.265 GHz and 1.49 GHz, i.e., 225 MHz. The Axial ratio BW is 16% with respect to design frequency of 1.375 GHz. At 1.375 GHz, axial ratio attains a minimum value of 0.031 dB. It confirms the circular polarization property at the design frequency.

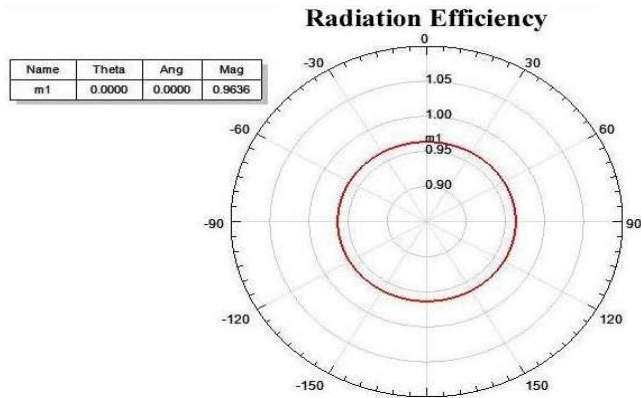


Figure 7. Simulated radiation efficiency.

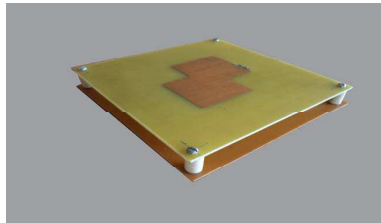


Figure 8. Photograph of the fabricated antenna.

Figure 7 shows the radiation efficiency of the designed antenna, computed using HFSS. The radiation efficiency is obtained as 0.9636 or 96.36%. The reduction in efficiency is due to lossy FR4 substrate. Also, the air gap between the substrate and ground plane influences the radiation pattern.

4. EXPERIMENTAL RESULTS

The prototype of the antenna is fabricated and the measurements are carried out by using Vector Network Analyzer E5062A for the parameters such as Return loss (dB), VSWR and smith plot.

Figure 8 shows the photograph of the fabricated antenna. Fig. 9 shows measured return loss (dB) Vs frequency graph. It shows that fabricated antenna is resonating at two frequencies, namely, 1.15 GHz (-13 dB) and 1.478 GHz (-21 dB). It is operating in the frequency band 1.1–1.17 GHz range (70 MHz). Also, it is operating well in the frequency range from 1.34 GHz–1.87 GHz, offering and impedance BW

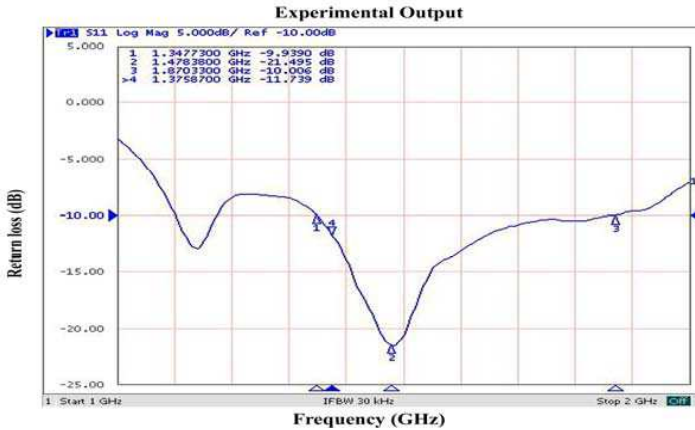


Figure 9. Measured return loss Vs frequency.

of 530 MHz. In both frequency bands, the return loss is below -10 dB. The resonant frequency is slightly shifted from 1.375 GHz to 1.478 GHz. This may be due to the following reasons:

- Instead of a metal ground plane, a PCB is used for fabrication in order to get the flat metal surface. So, the dielectric present in the top of PCB influences the effective dielectric constant and hence the resonant frequency is slightly deviated.
- The air gap between the ground plane and FR4 substrate is infinite in extent in x, y coordinates. Due to this, the gain of the antenna decreases and also the efficiency. Teflon is used as dielectric spacer for getting the air gap. It also influences the resonant frequency.
- In this type of antenna, the wideband is obtained at the expense of gain. In the receiving antenna, the low gain value is acceptable. But, transmission type antennas do not tolerate the gain value.

Figure 10 shows the measured VSWR graph ensures the above antenna operating in wideband in the frequency range from 1.34 GHz–1.87 GHz, and in the frequency band 1.1–1.17 GHz range (VSWR < 2). And If the threshold limit for VSWR is slightly increased to 2.5, then it covers the entire frequency range from 1.1–1.87 GHz (770 MHz). The percentage impedance BW in this case is 51.85%.

Figure 11 shows the measured input impedance Vs frequency in the range 1 GHz–2 GHz. At the resonance frequency, the input impedance is $42 - j1.74 \Omega$, which is close to line impedance 50Ω . From the graph, it is clear that the curve for input impedance is very close to unit circle. Hence, input matching is good at desired frequencies.

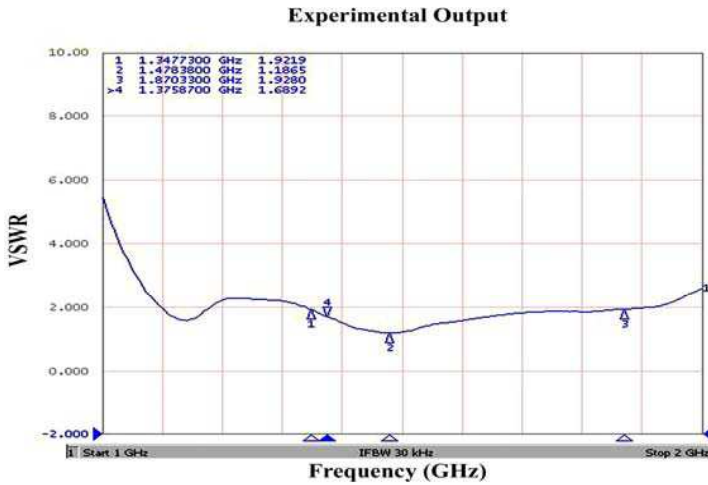


Figure 10. Measured VSWR Vs frequency.

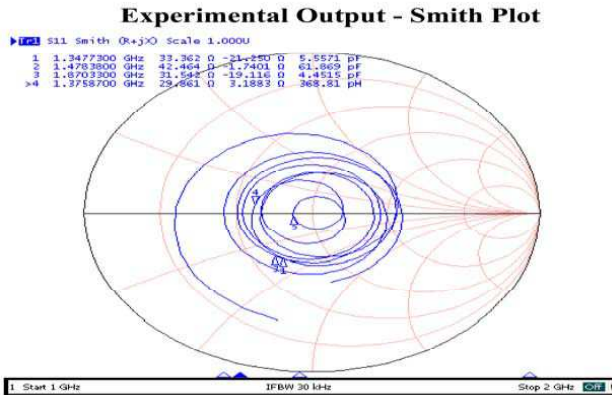


Figure 11. Measured input impedance Vs frequency.

The radiation pattern of the above wideband CP antenna is measured in an anechoic chamber. The test antenna is placed at the receiver side. The transmitting antenna is a standard gain horn antenna. The radiation pattern is measured in the frequency ranging from 1 GHz–2 GHz with spacing of 0.1 GHz. Fig. 12 shows the measured radiation pattern of wideband CP antenna at 1.575 GHz ($\varphi = 0$ degree) and ($\varphi = 90$ degree), i.e., L_1 frequency of GPS applications. In the ($\varphi = 0$) degree plane, peak received power is obtained as -48.42 dB and a 3 dB HPBW is obtained as 49.39 degrees. The test antenna is rotated by 90 degree to get ($\varphi = 90$ degree) cut

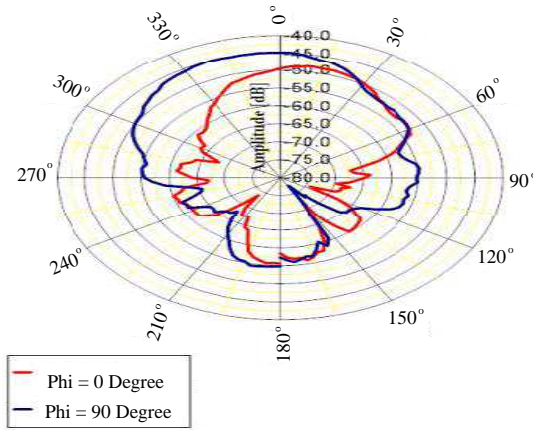


Figure 12. Measure radiation pattern at 1.575 GHz in both principal planes.

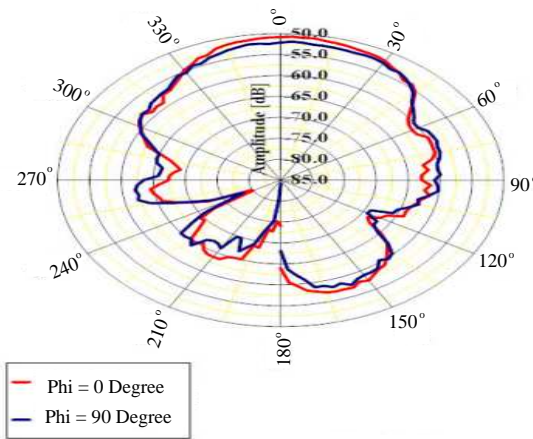


Figure 13. Measure radiation pattern at 1.2 GHz in both principal planes.

radiation pattern. In the ($\varphi = 90$ degree) cut, the peak received power is obtained as -44.69 dB and a 3 dB HPBW is obtained as 67.71 degrees. In both patterns, a wide beam width radiation pattern is obtained and also the beam is symmetric with respect to $\theta = 0$ degree. The front to back ratio in both planes at 1.575 GHz is approximately 10 dB.

Figure 13 shows the measured radiation pattern in both principal planes at 1.2 GHz, very close to L_2 and L_5 frequencies of GPS. The

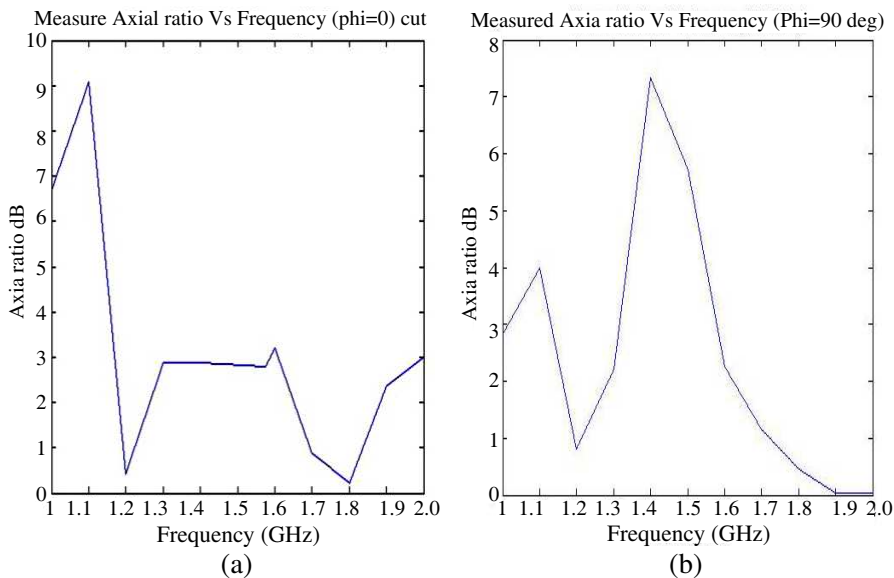


Figure 14. (a), (b) Measured axial ratio of wideband CP antenna ($\varphi = 0$ degree) cut and ($\varphi = 90$ degree) cut.

Table 3. Shows a comparison of simulation and experimental results.

Impedance Bandwidth		Axial Ratio (AR) Bandwidth ($\varphi = 0$ degree)	
Simulation VSWR < 2.5	Experimentally measured VSWR < 2.5	Simulation AR < 3 dB	Experimentally measured AR < 3 dB
1.15–1.6 GHz	1.1 GHz–1.87 GHz	1.26–1.49 GHz	1.15–1.8 GHz

beam peak power is obtained as -50.70 dB and 3 dB HPBW is 62.67 degrees in the ($\varphi = 0$) plane. The beam peak is obtained very close to the bore-sight axis. In the ($\varphi = 90$ degree) cut, a wide beam symmetrical radiation pattern is obtained. A 3 dB HPBW of 71 degree is obtained and beam peak is obtained as -51.88 dB. The front to back ratio at 1.2 GHz is approximately 16 dB in both planes. The radiation is mostly in the upper hemisphere, which is a requirement for a receiving antenna. The polarization performance is measured by axial ratio. The Axial ratio Vs Frequency plot is shown in Figs. 14(a), (b) for different frequencies at both principal planes given below.

The axial ratio is below 3 dB in the desired frequency range from 1.15–1.6 GHz to cover the L_1 , L_2 and L_5 frequencies of GPS. Hence,

Table 4. Shows comparison of simulated and measured results at desired frequencies.

Frequency (GHz)	Return loss (dB)		VSWR	
	Simulated	measured	Simulated	measured
1.575	-11	-14	1.77	1.5
1.227	-14.37	-9	1.45	2.2
1.176	-12.59	-13	1.58	1.4

circular polarization is obtained in the desired frequencies. A wide AR BW of 1.2–1.8 GHz is obtained.

Table 3 shows the comparison of simulated and measured results of impedance bandwidth and AR BW. From Table 3, it is clear that the antenna operates in wide frequency range. The desired frequency bands are covered in the operating range of the antenna.

Table 4 shows clear picture of impedance matching at the desired frequencies. The VSWR value is less than two in all the desired frequencies, which ensures the impedance matching of the antenna with line impedance.

5. CONCLUSION

Hence, a novel wideband circularly polarized antenna is designed, simulated, fabricated and tested. The truncated square MSA suspended over the ground plane with capacitive feed offers better impedance BW (VSWR < 2.5) in the frequency range 1.15–1.6 GHz, which includes the desired frequencies L_1 , L_2 and L_5 of GPS. It is better coincident with experimentally measured impedance bandwidth. The radiation pattern of above antenna is measured in an anechoic chamber. It radiates in the upper hemisphere of the antenna. An average HPBW of 60 degree is obtained in the measured radiation pattern. Also, the axial ratio is less than 3 dB in the frequency range 1.2–1.8 GHz. Also, this design approach provides enough freedom to the antenna engineer to tune any frequency range by varying the air gap, gap between feed strip and patch, dimensions of feed strip and truncating square size. It radiates in the upper hemisphere of antenna, which is the requirement for a CP receiving antenna. Hence, this antenna may be suitable for wideband circularly polarized receiving antenna applications.

ACKNOWLEDGMENT

The authors thank TARC, Thiagarajar College of Engineering, Madurai and Department of ECE, Anna university, Chennai for providing testing and computing facility respectively to complete the above work.

REFERENCES

1. Carver, K., "Microstrip antenna technology," *IEEE Trans. on Antennas and Propagation*, Vol. 29, No. 1, 2–24, 1981.
2. Kasabegowdar, V. G. and K. J. Vinoy, "Coplanar capacitive fed microstrip antenna for wideband applications," *IEEE Trans. on Antennas and Propagation*, Vol. 58, No. 10, 3131–3138, 2010.
3. Solanki, M. R., K. Usha Kiran, and K. J. Vinoy, "Broadband design of a triangular microstrip antenna with a capacitive feed," *Journal of Microwaves, Optoelectronics and Electromagnetic Applications*, Vol. 7, No. 8, 44–53, 2008.
4. Kasabegowdar, V. G. and K. J. Vinoy, "A wideband microstrip antenna with symmetric radiation pattern," *Microwave and Optical Technology Letters*, Vol. 50, No. 8, 1991–1995, 2008.
5. Yang, S. S., K.-F. Lee, A. A. Kishk, and K.-M. Luk, "Design and study of single fed wideband circularly polarized microstrip antenna," *Progress In Electromagnetics Research*, Vol. 80, 45–61, 2008.
6. Kasabegowdar, V. G. and K. J. Vinoy, "A broadband suspended microstrip antenna for circular polarization," *Progress In Electromagnetic Research*, Vol. 90, 353–368, 2009.
7. Kasabegowdar, V. G., "Low profile suspended microstrip antennas for wideband applications," *Journal of Electromagnetic Waves and Applications*, Vol. 25, No. 13, 1795–1806, 2011.
8. Rao, P. N. and N. V. S. N. Sarma, "A single feed circularly polarized fractal shaped microstrip antenna with fractal slot," *PIERS Proceedings*, 95–197, Hangzhou, China, Mar. 24–28, 2008.
9. Murugan, S. and V. Rajamani, "Design of wideband circularly polarised capacitive fed microstrip antenna," *Int. Conf. on Communication Technology and System Design, ICCTSD*, 382–389, Procedia Engineering, Dec. 7–9, 2011.
10. Padros, N., J. L. Ortgosu, and J. Baker, "Comparative study of high performance GPS receiving antenna designs," *IEEE Trans. on Antennas and Propagation*, Vol. 45, No. 4, 698–706, 1997.
11. Tranquilla, J. M. and S. R. Best, "A study of Quadrafilal Helix

- antenna for global position systems applications,” *IEEE Trans. on Antennas and Propagation*, Vol. 38, No. 10, 1545–1550, 1990.
12. Boccia, L., G. Amendola, and G. D. Mossa, “A shorted elliptical patch antenna for GPS applications,” *IEEE Trans. on Antennas and Propagation*, Vol. 2, No. 1, 6–8, 2003.
 13. Boccia, L., “A Dual frequency microstrip antenna for high precision GPS applications,” *IEEE Antennas and Wireless Propagation Letters*, Vol. 3, No. 1, 157–160, 2004.
 14. Wang, Y.-S. and S.-J. Chung, “A miniature quadrafilar helix antenna for global positioning satellite reception,” *IEEE Trans. on Antennas and Propagation*, Vol. 57, No. 12, 3746–3751, 2009.
 15. Serra, A. A., P. Nepa, G. Manara, and R. Massini, “A low profile linearly polarised 3D PIFA for handheld GPS terminals,” *IEEE Trans. on Antennas and Propagation*, Vol. 58, No. 4, 1060–1066, 2010.
 16. Scire-Scappuzzo, F. and S. N. Markov, “A Low profile multipath wideband GPS antenna with cutoff or non-cutoff corrugated ground planes,” *IEEE Trans. on Antennas and Propagation*, Vol. 57, No. 1, 33–46, 2009.
 17. Kumar, G. and K. P. Ray, *Broadband Microstrip Antennas*, Artech House, 2003.
 18. Bhal, I. J. and P. Bhartia, *Microstrip Antennas*, Artech House, 1980.
 19. Bird, T. S., “Definition and misuse of return loss,” *IEEE Trans. on Antennas and Propagation Magazine*, Apr. 2009.